One-Electron Spectral Weight of the Doped Two-Dimensional Hubbard Model

N. Bulut,[1] D. J. Scalapino,[2] and S. R. White[3]

[1]*Department of Physics, University of Illinois, Urbana, Illinois 61801-3080*
[2]*Department of Physics, University of California, Santa Barbara, California 93106-9530*
[3]*Department of Physics, University of California, Irvine, California 92717-4575*

(Received 14 October 1993)

We have calculated the single-particle density of states $N(\omega)$ and the spectral weight $A(\mathbf{p},\omega)$ for the doped two-dimensional Hubbard model by combining quantum Monte Carlo simulations with the maximum-entropy analytic continuation technique. We present results for various values of the doping, temperature, and Coulomb repulsion U. For sufficiently strong Coulomb repulsions and near half filling, a Mott-Hubbard pseudogap exists. In this case, we find that a peak develops at the top of the lower Hubbard band near the Fermi level at temperatures of order the hopping t. The structure of this peak is similar to that seen in the infinite-dimensional Hubbard model.

PACS numbers: 71.27.+a, 74.20.Mn

Photoemission spectroscopy [1–5] provides important information on the one-electron density of states $N(\omega)$ and angular resolved spectroscopy can in principle probe the spectral weight $A(\mathbf{p},\omega)$. Numerical results from band structure calculations [6] give important information on the shape of the Fermi surface. However, these calculations do not take into account dynamic correlations produced by the electron-electron interactions which are thought to play an essential role in determining the spectral weight distribution in strongly correlated systems such as the cuprates or the heavy fermion systems. Various approximate many-body calculations [7,8] as well as phenomenological suggestions [9] have been made for the structure of $N(\omega)$ and $A(\mathbf{p},\omega)$; however, it is difficult to determine the validity of these because of the absence of a small parameter or exact results with which to compare. One method which has proved useful is the exact diagonalization of small clusters. For example, the spectral weight and density of states have been calculated for 4×4 Hubbard clusters [10,11]. However, here questions of lattice size and degeneracy have been raised and one would like to obtain results for larger clusters. One approach, applied successfully to the half-filled two-dimensional Hubbard model [12–14], involves combining finite temperature quantum Monte Carlo techniques [15] with maximum entropy [16] estimates to obtain $N(\omega)$ and $A(\mathbf{p},\omega)$. Here, we extend this approach to the two-dimensional Hubbard model doped away from half filling [17]. Specifically, we present results for $N(\omega)$ and $A(\mathbf{p},\omega)$ for 8×8 lattices with various values of the filling $\langle n\rangle$, temperature, and on-site Coulomb interaction U.

For a strong Coulomb interaction (U of order the bandwidth) we find in agreement with previous studies [10,18] that when the system is doped, the chemical potential shifts from the center of the gap, appropriate to the half-filled system, to near the top edge of the lower Hubbard band. In addition, spectral weight is transferred to the upper part of the lower band extending out to form a pseudogap region. Furthermore, a peak in $N(\omega)$ is formed on the upper part of the lower band near the Fermi energy. A number of these same features appear in the exact diagonalization studies of the 4×4 cluster [10] as well as in recent work on the infinite-dimensional Hubbard model [19,20]. We believe that these results are therefore not artifacts of small lattices, but rather represent the physical effects of strong electron-electron correlations. They provide a useful testing ground for approximate theories and a reference for the type of behavior which should be observed in photoemission of strongly correlated materials.

Here we study the Hubbard Hamiltonian

$$H=-t\sum_{\langle ij\rangle,\sigma}(c_{i\sigma}^{\dagger}c_{j\sigma}+c_{j\sigma}^{\dagger}c_{i\sigma})+U\sum_{i}n_{i\uparrow}n_{i\downarrow} \tag{1}$$

on a two-dimensional square lattice. The operator $c_{i\sigma}^{\dagger}$ creates an electron of spin σ on site i and $n_{i\sigma}=c_{i\sigma}^{\dagger}c_{i\sigma}$. There is a near neighbor hopping t and an on-site repulsive interaction U. A chemical potential μ is used to set the filling $\langle n\rangle=\langle n_{i\uparrow}+n_{i\downarrow}\rangle$. Using Monte Carlo techniques [15], we have calculated the single-particle finite temperature Green's function

$$G_{ij}(\tau)=-\langle T_{\tau}c_{j\sigma}(\tau)c_{i\sigma}^{\dagger}(0)\rangle . \tag{2}$$

Here the expectation value is the trace over the grand canonical ensemble and $c_{j\sigma}(\tau)=\exp[\tau(H-\mu N)]c_{j\sigma}\times\exp[-\tau(H-\mu N)]$ is the usual imaginary-time dependent operator. By Fourier transforming on $\mathbf{j}-\mathbf{i}$ we obtain $G(\mathbf{p},\tau)$ which for $\tau>0$ is related to the spectral weight by

$$G(\mathbf{p},\tau)=-\int_{-\infty}^{+\infty}d\omega\frac{A(\mathbf{p},\omega)e^{-\tau\omega}}{1+e^{-\beta\omega}} . \tag{3}$$

As previously described [12–14,16], a maximum entropy estimate can be used to invert Eq. (3) and obtain $A(\mathbf{p},\omega)$. Likewise data on $G_{ii}(\tau)$ give the density of states $N(\omega)$. As is known, such calculations require high quality data. The results reported here have been obtained by making over 10^5 updates of all the Hubbard-Stratonovich variables, and $G(\mathbf{p},\tau)$ had statistical error less than 0.5%. As discussed in Refs. [12–14], various

0031-9007/94/72(5)/705(4)$06.00

moments of the spectral weights were also made use of in carrying out the analytic continuation with the maximum entropy technique. In order to have a check on the maximum entropy technique, we have also calculated $N(\omega)$ and $A(\mathbf{p},\omega)$ using Padé approximants. This crude but simpler method gave results in good agreement with those reported here. These comparisons and other tests of the maximum entropy technique will be discussed elsewhere [21].

All of the following results are for 8×8 lattices, except in Fig. 2, where we show data obtained on a 4×4 lattice for the purpose of estimating the finite size effects. In Figs. 1(a)-1(c), $N(\omega)$ versus ω is shown for $U=8t$ at half filling, at $\langle n\rangle=0.87$ corresponding to small doping, and at $\langle n\rangle=0.70$ in the overdoped regime. The solid line in Fig. 1(a) is the noninteracting density of states at half filling given by $N(\omega)=(1/2\pi^2 t)K(\sqrt{1-(\omega/4t)^2})$ where K is the elliptic integral of the first kind. The rest of the curves in Fig. 1(a) are for $U=8t$ and $\langle n\rangle=1.0$ at various temperatures. For this value of U, a Mott-Hubbard pseudogap exists at high temperatures [14]. As the temperature is lowered and the antiferromagnetic correlations extend across the 8×8 lattice, a spin-density-wave (SDW) Mott-Hubbard gap opens. For the infinite lattice, SDW long-range order occurs at $T=0$; however, the Mott-Hubbard pseudogap develops at finite temperatures [13, 14].

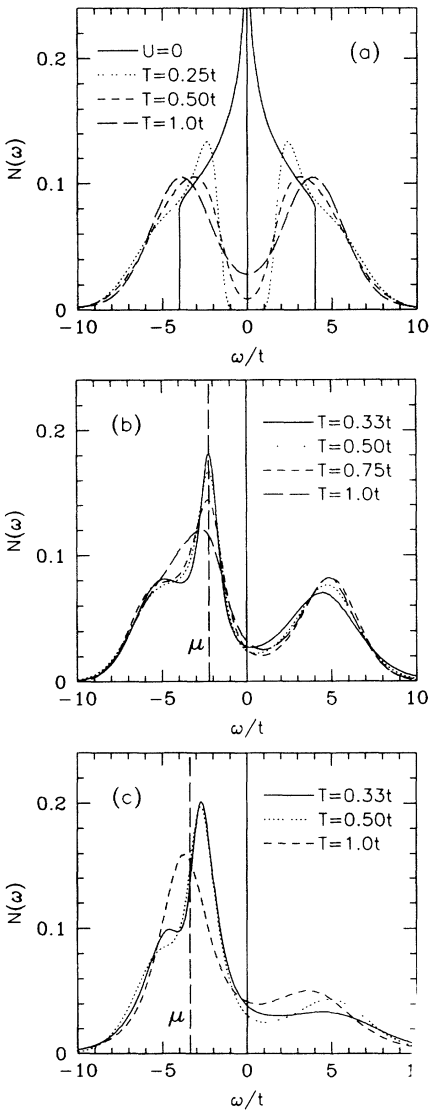

FIG. 1. Density of states $N(\omega)$ versus ω on an 8×8 lattice for $U=8t$, various temperatures, and (a) $\langle n\rangle=1.0$, (b) $\langle n\rangle=0.87$, and (c) $\langle n\rangle=0.70$. In (a) the solid curve is the $U=0$ density of states, and the rest of the curves are for $U=8t$ at various temperatures. In (b) and (c), the long-dashed vertical line denotes the chemical potential μ for the lowest temperature $T=0.33t$. Here $N(\omega)$ is plotted in units of t^{-1}.

In Fig. 1(b), $N(\omega)$ is shown at $\langle n\rangle=0.87$ for various temperatures. Upon doping the chemical potential shifts by a substantial amount, and the Mott-Hubbard pseudogap continues to exist [10]. In addition, a peak starts to develop at the top of the lower Hubbard band as T is lowered from t to $0.75t$. The chemical potential is near this peak and the low lying single-particle excitations are associated with the states in this peak. At lower temperatures this peak sharpens and has a width of order t. For this filling, the lowest temperature at which we have carried out simulations on the 8×8 lattice is $T=0.33t$, where the average sign of the fermion determinants [22] is about 0.35. Here we are in a temperature regime where the average sign is falling very rapidly, hence lower temperatures require much longer simulation times. For instance, it is beyond our computational resources to calculate $N(\omega)$ at $T=0.25t$ on the 8×8 lattice using the current Monte Carlo algorithm.

Figure 1(c) shows $N(\omega)$ at $\langle n\rangle=0.70$ in the overdoped regime for various temperatures. Here we see that the Fermi level has moved further away from the peak and the pseudogap is washed out.

In order to have an estimate of the finite size effects on $N(\omega)$, in Fig. 2 we show results obtained on a 4×4 lattice

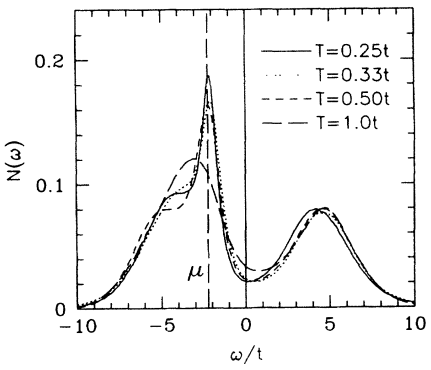

FIG. 2. Density of states $N(\omega)$ versus ω on a 4×4 lattice for $U=8t$, $\langle n\rangle=0.87$, and various temperatures.

with $U=8t$ and $\langle n\rangle=0.87$. On the 4×4 lattice, the sign problem is less severe and we have carried out simulations down to $T=0.25t$, where the average sign is 0.2. Comparing Figs. 1(b) and 2, we observe that the finite size effects are small, which is reasonable since these calculations have been carried out at relatively high temperatures.

Figure 3 illustrates what happens for a smaller value of the Coulomb repulsion, $U=4t$, at 0.87 filling. In this case, there is little evidence for a pseudogap, but a peaked structure near the chemical potential remains.

The results on $N(\omega)$ that we have presented here for the two-dimensional Hubbard model are very similar to those obtained by Jarrell [19] in the limit of infinite dimensions. In this limit, the single-particle self-energy becomes local [23,24], and hence one can exactly map the problem to the single-impurity Anderson model [19]. Just as here, in $d=\infty$ a Mott-Hubbard gap opens at half filling [19,20]. Upon doping a pseudogap remains, and a peak at the top of the lower Hubbard band grows as T is lowered [19,20]. Since in $d=\infty$ the problem can be mapped to the single-impurity Anderson model, this peak corresponds to an Abrikosov-Suhl resonance associated with the screening of the impurity magnetic moment by the Fermi sea. The remarkable similarity of $N(\omega)$ for $d=2$ to that of $d=\infty$ suggests that a similar type of physics takes place in the $d=2$ Hubbard model. This would then mean that the peak in $N(\omega)$ seen in Fig. 1(b) is a virtual bound state, and is due to the screening of the large magnetic moments formed by the strong on-site Coulomb repulsion.

In order to have a closer look at the formation of the peak in $N(\omega)$, we present results on the single-particle spectral weight, $A(\mathbf{p},\omega)=(-1/\pi)\mathrm{Im}G(\mathbf{p},\omega)$, at $\mathbf{p}=(\pi/2,\pi/2)$ for $\langle n\rangle=0.87$. Figures 4(a) and 4(b) show $A(\mathbf{p},\omega)$ versus ω for $U=8t$ and $4t$, respectively, at various temperatures. For the noninteracting system, the $\mathbf{p}=(\pi/2,\pi/2)$ point lies about $0.3t$ above the Fermi level. Here we see that for $U=8t$ and at high temperatures, the spectral weight is pushed well below the Fermi level because of the Mott-Hubbard pseudogap. However, as T is lowered, the spectral weight shifts towards the Fermi level, forming the peak in $N(\omega)$. We have found similar temperature dependence for other points near the $U=0$ Fermi surface, for instance, $\mathbf{p}=(3\pi/4,0)$ or $\mathbf{p}=(\pi,0)$. As seen in Fig. 4(b), for $U=4t$, $A(\mathbf{p},\omega)$ at $\mathbf{p}=(\pi/2,\pi/2)$ is always peaked at positive frequencies, apparently because there is no Mott-Hubbard pseudogap. On the other hand, $A(\mathbf{p}=(3\pi/4,0),\omega)$ peaks for $\omega<0$. From the locations of the peaks in $A(\mathbf{p},\omega)$ on the 8×8 lattice, we have estimated the shape of the Fermi surface by interpolation and found that it resembles that of the noninteracting system. However, for $U=8t$, $A(\mathbf{p},\omega)$ is still shifting at these temperatures and it is not possible to estimate the shape of the Fermi surface.

In summary, we have presented results on the single-particle density of states and the spectral weight of the two-dimensional Hubbard model obtained from maximum-entropy analytic continuation of Monte Carlo data. We reported results for different values of the doping, temperature, and Coulomb repulsion U. For the $U=8t$ case, the Mott-Hubbard pseudogap continues to exist for fillings close to $\langle n\rangle=1.0$. In addition, in this case, a peak develops at the top of the lower Hubbard band for temperatures less than the hopping t. Its similarity to what is observed in the $d=\infty$ Hubbard model suggests that this resonance in the single-particle spectrum represents a vir-

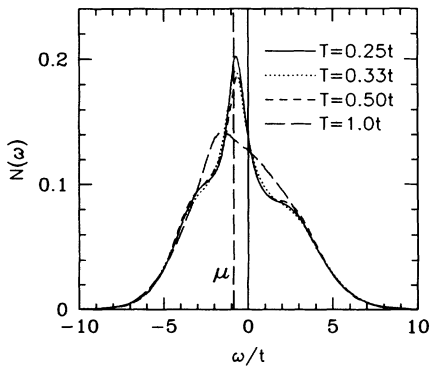

FIG. 3. Density of states $N(\omega)$ versus ω on an 8×8 lattice for $U=4t$, $\langle n\rangle=0.87$, and various temperatures.

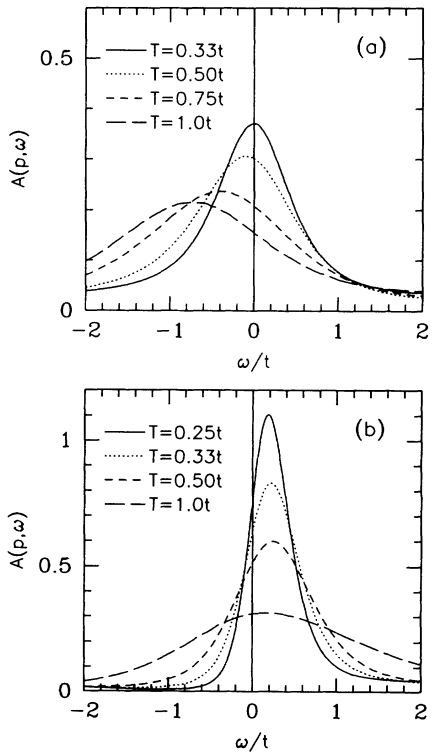

FIG. 4. Spectral weight $A(\mathbf{p},\omega)$ versus ω at $\mathbf{p}=(\pi/2,\pi/2)$ for $\langle n\rangle=0.87$, various temperatures, and (a) $U=8t$ and (b) $U=4t$. Here $\omega=0$ corresponds to the chemical potential.

tual bound state, and that it is due to the screening of the large magnetic moments forming at each lattice site. For a weaker Coulomb repulsion such as $U=4t$, a pseudogap is not observed at these temperatures, and the density of states looks more similar to that of the noninteracting system. The results for $N(\omega)$ and $A(\mathbf{p},\omega)$ are also similar in many respects to the 4×4 exact diagonalization calculations [10], suggesting that a consistent picture for the one-electron spectral weight of the Hubbard model is emerging [25]. We note, however, that this picture in which the chemical potential switches across the Mott-Hubbard gap and spectral weight is transferred to the top (bottom) of the lower (upper) Hubbard band under hole (electron) doping is very different than the interpretation of some of the photoemission spectroscopy results [3,26]. This implies that either there is essential physics missing from the Hubbard model which is required to describe the cuprates or that surface effects or Madelung energy changes enter the experimental results.

We thank J. Allen, M. Jarrell, and Z. X. Shen for helpful discussions. N.B. would like to acknowledge support by the National Science Foundation (DMR 91-20000) through the Science and Technology Center for Superconductivity, and D.J.S. would like to acknowledge support for this work from the Department of Energy under Grant No. DE-FG03-85ER45197. S.R.W. would like to thank the office of Naval Research for support under Grant No. N00014-91-J-1143. The numerical calculations reported in this paper were performed at the San Diego Supercomputer Center.

[1] Z.-X. Shen *et al.*, Phys. Rev. B **36**, 8414 (1987); Z.-X. Shen *et al.*, Phys. Rev. Lett. **64**, 2442 (1990).
[2] C. G. Olson *et al.*, Science **245**, 731 (1989).
[3] J. W. Allen *et al.*, Phys. Rev. Lett. **64**, 595 (1990).
[4] J. C. Campuzano *et al.*, Phys. Rev. Lett. **64**, 2308 (1990).
[5] T. Takahashi *et al.*, Physica (Amsterdam) **170C**, 416 (1990).
[6] R. E. Cohen, W. E. Pickett, and H. Krakauer, Phys. Rev. Lett. **62**, 831 (1989).
[7] A. Kampf and J. R. Schrieffer, Phys. Rev. B **41**, 6399 (1990); **42**, 7967 (1990).
[8] P. W. Anderson, Phys. Rev. Lett. **64**, 839 (1990).
[9] C. M. Varma *et al.*, Phys. Rev. Lett. **63**, 1996 (1989).
[10] E. Dagotto, A. Moreo, F. Ortolani, J. Riera, and D. J. Scalapino, Phys. Rev. Lett. **67**, 1918 (1991); E. Dagotto, J. Riera, and D. J. Scalapino, Phys. Rev. B **46**, 3183 (1992).
[11] D. J. Scalapino, Physica (Amsterdam) **185-189C**, 104 (1991).
[12] S. R. White, Phys. Rev. B **44**, 4670 (1991).
[13] S. R. White, Phys. Rev. B **46**, 5678 (1992).
[14] M. Vekic and S. R. White, Phys. Rev. B **47**, 1160 (1993).
[15] S. R. White, D. J. Scalapino, R. L. Sugar, E. Y. Loh, J. E. Gubernatis, and R. T. Scalettar, Phys. Rev. B **40**, 506 (1989).
[16] R. N. Silver, D. S. Sivia, and J. E. Gubernatis, Phys. Rev. B **41**, 2380 (1990).
[17] Preliminary results on this work have been reported in Ref. [11].
[18] N. Furukawa and M. Imada, J. Phys. Soc. Jpn. **60**, 3604 (1991).
[19] M. Jarrell, Phys. Rev. Lett. **69**, 168 (1992).
[20] M. Jarrell and Th. Pruschke, Z. Phys. B **90**, 187 (1993).
[21] N. Bulut, D. J. Scalapino, and S. R. White (unpublished).
[22] For a recent review of the sign problem and the Monte Carlo technique used here see D. J. Scalapino, in Proceedings of the Summer School on Modern Perspectives in Many-Body Physics, Canberra, January 1993 (World Scientific, Singapore, to be published).
[23] W. Metzner and D. Vollhardt, Phys. Rev. Lett. **62**, 324 (1989).
[24] E. Müller-Hartmann, Z. Phys. B **74**, 507 (1989).
[25] It is also interesting to compare these results with the recent results on the one-dimensional Hubbard model obtained by M. Gulacsi and K. S. Bedell [Physica (Amsterdam) B (to be published)], and by R. Preuss, A. Muramatsu, W. von der Linden, F. F. Assaad, and W. Hanke (to be published).
[26] R. O. Anderson *et al.*, Phys. Rev. Lett. **70**, 3163 (1993).